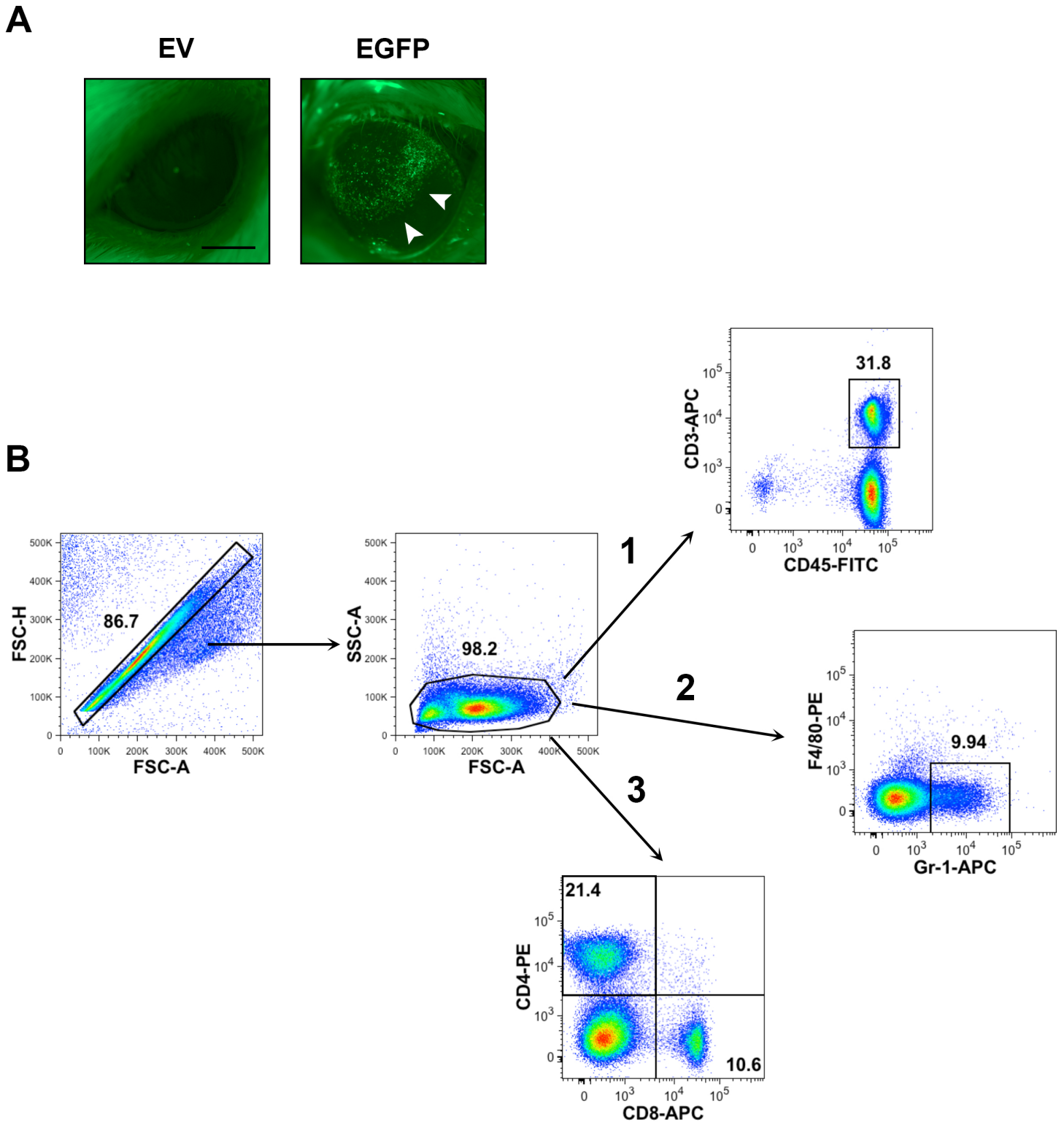
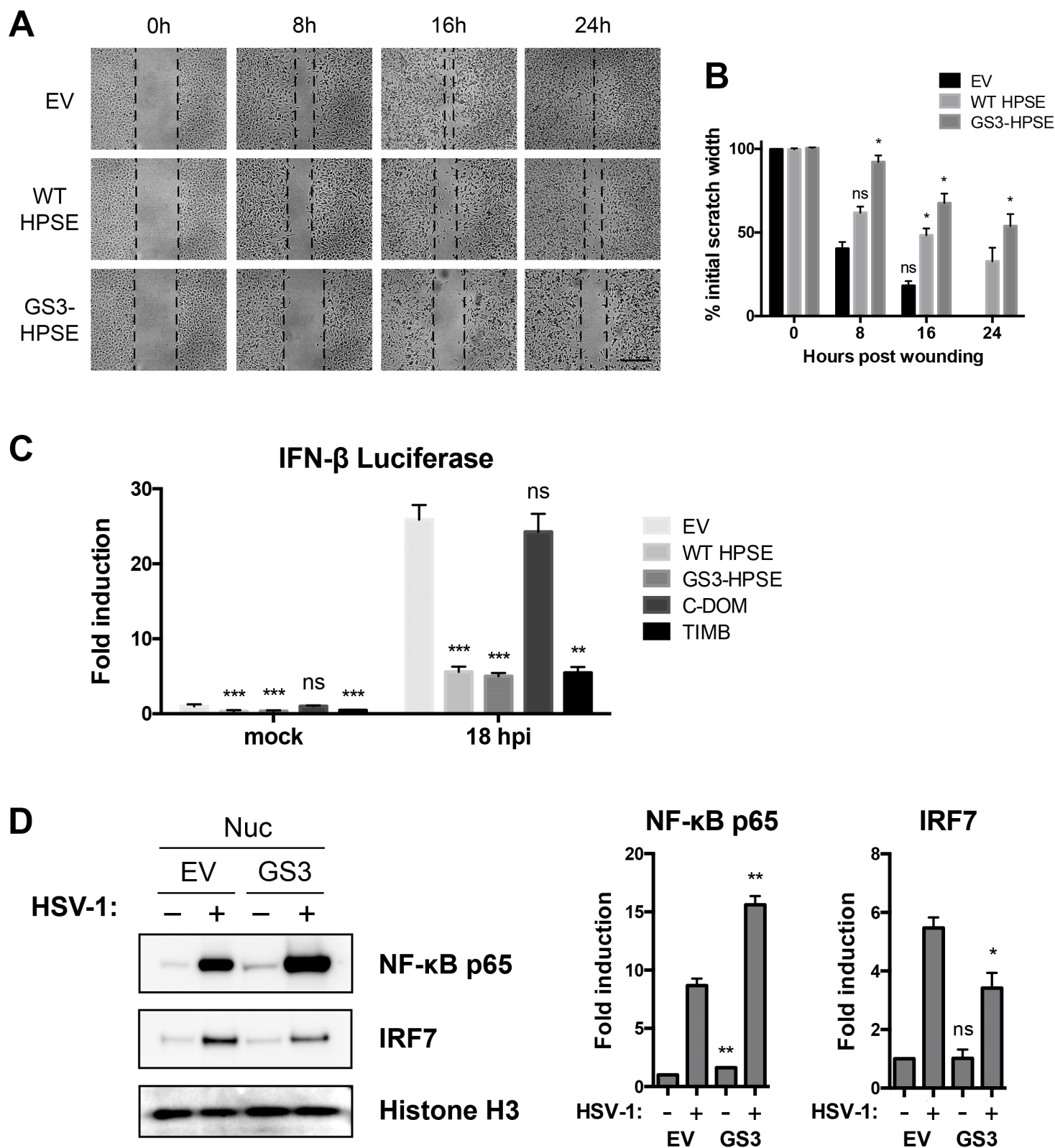


**Figure S1 | Normal HPSE biogenesis and variants used in this study. Related to Figures 1-4.** **A**, HPSE is produced as a preproprotein containing a signal sequence that is cleaved by signal peptidase to yield an inactive 65-kDa proHPSE. Removal of the intervening linker by Cathepsin L yields active HPSE, a heterodimer composed of 50-kDa and 8-kDa subunits. **B**, To study the effect of HPSE in promoting viral pathogenesis, we employed several plasmids encoding variants of the human HPSE gene. Of major focus in this work is the “GS3” form, in which the linker of the inactive 65-kDa form is replaced with a triple repeat of Gly-Ser to produce a constitutively active HPSE. **C**, Expression of each of these HPSE variants in HCE cells was observed by western blot using antibodies specific against human HPSE.



**Figure S2 | Corneal transfection and flow cytometry gating strategy. Related to Figure 1. A**, Efficiency of murine corneal transfection is demonstrated with the use of EGFP plasmid compared to empty vector. Representative stereoscope images show detection of EGFP in transfected corneas (arrowheads). Scale bar, 1 mm. **B**, Representative composite depicting gating strategy for flow cytometric analysis of ipsilateral draining lymph node (submandibular).



**Figure S3 | GS3-HPSE overexpression in HeLa cells delays wound healing, inhibits type I interferon signaling, and enhances NF- $\kappa$ B nuclear translocation. Related to Figures 2-4. A, Representative micrographs of *in vitro* wound healing assay showing closure of HeLa cellular defect over specified times after scratching. Before wound application, cells were transfected with empty vector, WT HPSE or GS3-HPSE. Scale bar, 50  $\mu$ m. B, Quantification of extent of wound healing in A. Pixel distances between wound fronts in each panel were measured, and percentages of initial wound widths are depicted. C, Luciferase assay results from HeLa cells co-transfected with HPSE variants and pNF- $\kappa$ B-luc or pIFN $\beta$ -luc plasmids. D, Nuclear extracts of HeLa cells transfected with empty vector or GS3-HPSE in absence or presence of HSV-1 (KOS MOI 0.1) for 24 h. Means  $\pm$  SEM of three independent experiments ( $n=3$ ) are plotted. Asterisks denote a significant difference compared to EV, as determined by Student's *t*-test; \* $P<0.05$ , \*\* $P<0.01$ , \*\*\* $P<0.001$ , ns, not significant.**

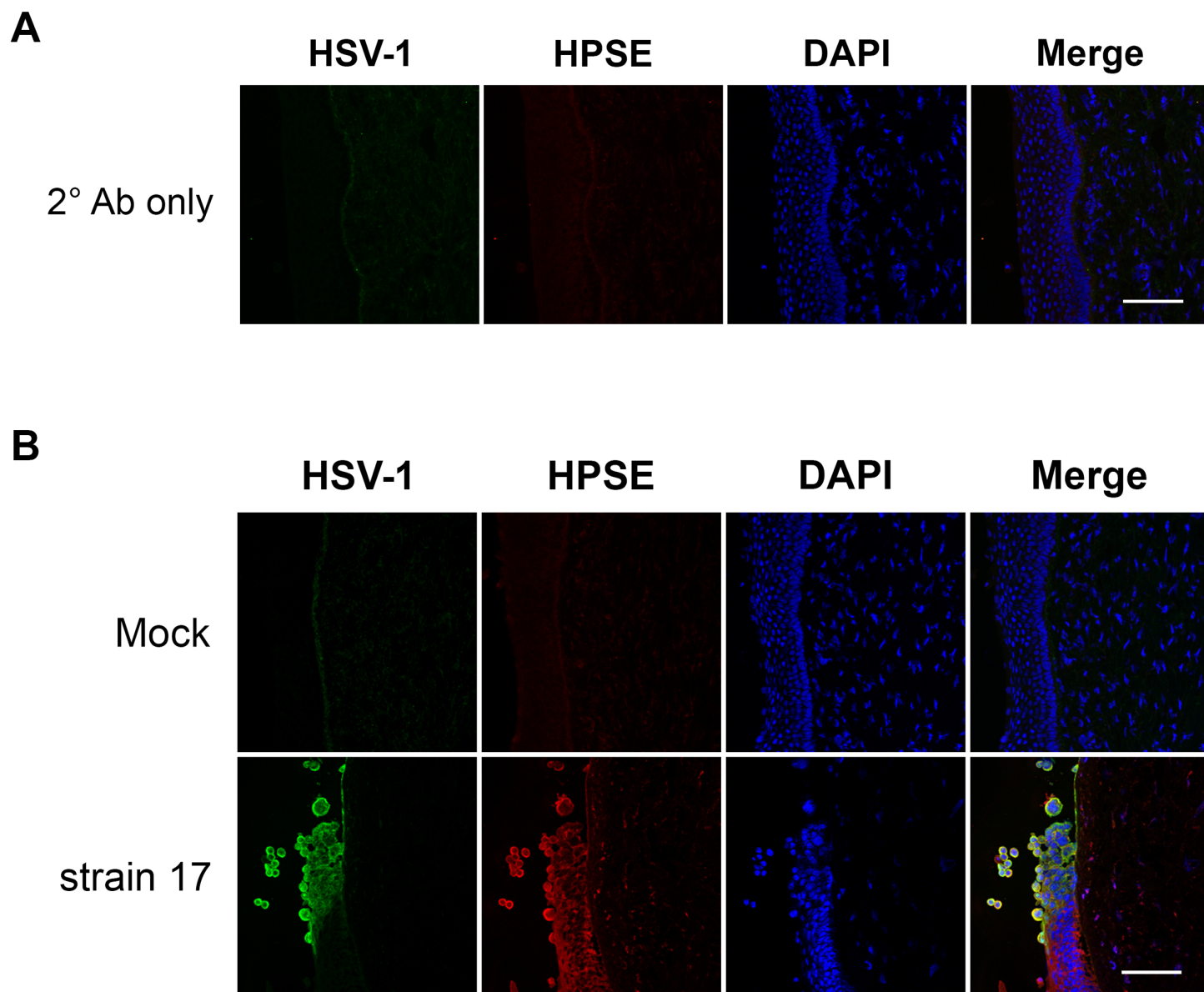


**Figure S4 | Staining controls for immunohistochemistry of porcine corneas. Related to Figure 5.** **A**, Secondary antibody only control. Corneal tissue was infected with strain 17 and immunohistochemistry protocol was followed with no addition of primary antibodies. Scale bar, 100  $\mu$ m. **B**, Mock control. Porcine corneas were incubated with HSV-1 (strain 17) or without virus (Mock), processed and stained following immunohistochemistry protocol. Scale bar, 100  $\mu$ m.



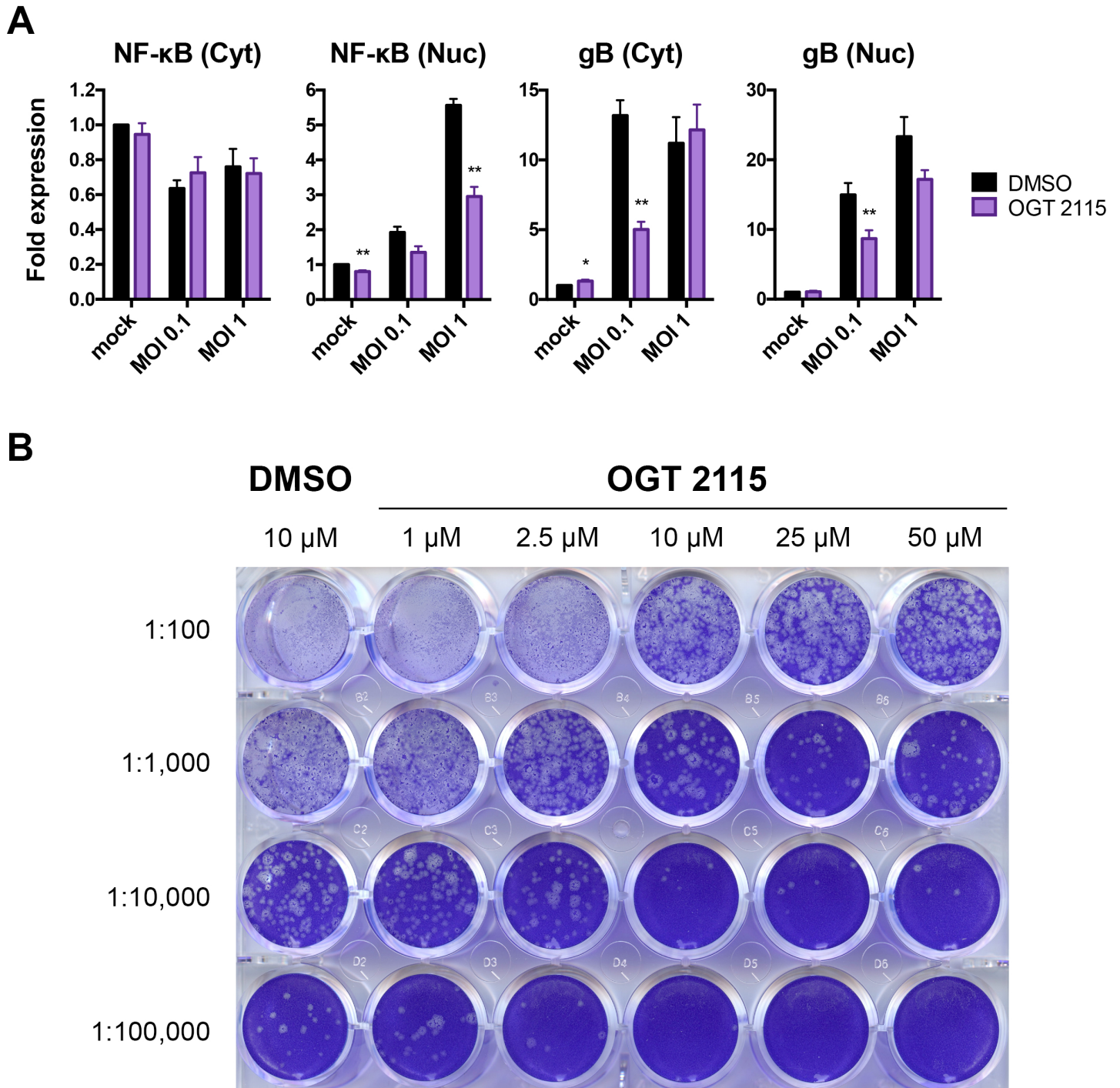


**Figure S5 | Pharmacological inhibition of HPSE with OGT 2115 decreases NF-κB translocation to nucleus, viral glycoprotein production and viral release. Related to Figure 6. A,** Quantification of western blot represented in Figure 5C. Fold expression over DMSO mock normalized to respective control (GAPDH for cytosolic, Histone H3 for nuclear). Means  $\pm$  SEM of three independent experiments ( $n=3$ ) are plotted. Asterisks denote a significant difference compared to respective DMSO sample, as determined by Student's  $t$ -test; \* $P<0.05$ , \*\* $P<0.01$ , \*\*\* $P<0.001$ , ns, not significant. **B,** Full-plate image of representative plaque assay. Confluent Vero cells were inoculated with dilutions of supernatants of HCE cells previously infected with HSV-1 (KOS MOI 0.1) for 2 h then incubated with the specified concentrations of DMSO or OGT 2115 for 24 h. Crystal violet staining pattern is shown.

